

Thermodynamic and Electrochemical investigation of (9-[(R) 2[[bis [[(isopropoxycarbonyl)oxy]methoxy] phosphinyl] methoxy] propyl] adenine fumarate) as Green Corrosion Inhibitor for Mild Steel in 1M HCl

Garima Shahi¹, Chandra Bhan Verma², E.E. Ebenso³, M.A.Quraishi^{2,*}

¹ Department of Chemical Engineering and Technology, , Banaras Hindu University, Varanasi 221005, India

² Department of Chemistry, Indian Institute of Technology, Banaras Hindu University, Varanasi 221005, India

³ Material Science Innovation & Modelling (MaSIM) Research Focus Area, Faculty of Agriculture, Science and Technology, North-West University (Mafikeng Campus), Private Bag X2046, Mmabatho 2735, South Africa

*E-mail: maquraishi.apc@itbhu.ac.in, maquraishi@rediffmail.com

Received: 18 October 2014 / Accepted: 7 December 2014 / Published: 16 December 2014

Corrosion inhibition property of [(9-[(R) 2 [[bis [[(isopropoxycarbonyl) oxy] methoxy] phosphinyl] methoxy] propyl] adenine fumarate)] (Tenvir) on mild steel in 1M HCl have been investigated using chemical and electrochemical methods. The Tenvir acts as efficient corrosion inhibitor for mild steel in 1M HCl and its inhibition efficiency increases on increasing concentration. Potentiodynamic polarization study revealed that Tenvir effectively suppressed both the anodic and cathodic processes of mild steel corrosion in acid solution and behaves as mixed-type inhibitor. Formation of the protective film of this Tenvir on mild steel surface was studied by Scanning electron microscopy (SEM) and energy dispersive X-ray spectroscopy (EDX) techniques. Adsorption of the Tenvir on the mild steel surface in acid solution was found to obey the Langmuir adsorption isotherm. Effect of temperature on the inhibition efficiency was also investigated and some thermodynamic parameters were calculated in order to explain the mechanism of adsorption.

Keywords: mild steel, acid solution, EIS, Tafel polarization, SEM/EDX, Tenvir

1. INTRODUCTION

Corrosion is the deterioration of materials by chemical interaction with their environment. The term corrosion is sometimes use for the degradation of plastics, concrete and wood, but generally

refers to metals. Mild steel is very reactive material and prone to corrosion in acid media [1]. The corrosion inhibition of metal can be best achieved by application of organic corrosion inhibitors. The efficiency of organic inhibitors depends on the nature of environment, nature of metal, structure of inhibitor, electrochemical potential at the metal/ electrolyte interface, which includes number of adsorption centers in the molecule, their charge density, the molecular size, and mode of adsorption, formation of metallic complexes and the projected area of inhibitor on the metal surface. The choice of organic compounds as corrosion inhibitor is based on the consideration that these contain conjugated pi-electrons and heteroatoms which provide them a better coordination and adsorption property. The adsorption of these compounds is influenced by the electronic structure of inhibitor molecules, steric factor, aromatic and electron density at donor site, presence of functional groups such as $-CHO$, $-N=N$, $R-OH$ etc. molecular weight and molecular area of inhibitor molecule [2-5]. Most of the organic inhibitors are toxic, highly expensive and environment unfriendly. In recent times research activities are focused towards developing the cheap, nontoxic and environment friendly corrosion inhibitor. Thus it is important and desirable to develop the novel corrosion inhibitors of natural source and non-toxic type. Due to their natural origin and non toxic nature drugs are ideal candidature to replace the traditional toxic organic corrosion inhibitors. The literature survey reveals that following drugs were used as efficient corrosion inhibitors for mild steel corrosion in acidic solution: Ceftriaxone, Cefalexin, Doxycycline, Pheniramine, Fexofenadine, Ceftobiprole, Ranitidine, Rhodanine azosulpha, Dapsone, Mebendazole, Penicillin G, Penicillin V potassium, Ciprofloxacin, Cefadroxil, Ampicillin, Sparfloxacin, Chloramphenicol, Ketoconazole, Orphenadrine, Cefotaxime, Methocarbamol, Metformin, Cefazolin, Cloxacillin, Nitrofurantoin and Abacavir [6-21].

In present study, we have reported corrosion inhibition property of Tenvir in 1M HCl using gravimetric and electrochemical methods. Tenvir is manufactured by Cipla Pharma Limited (India) having the IUPAC name (9-[(R) 2[[bis [[(isopropoxycarbonyl)oxy]methoxy] phosphinyl] methoxy] propyl] adenine fumarate). The chemical structure of the Tenvir is given in Figure1. The molecular formula is $C_{19}H_{30}N_5O_{10}P$. $C_4H_4O_4$ and Molecular mass is 635.51 g/mol. The LD50 dose of Tenvir is > 1500 mg/kg for Rat suggesting that Tenvir is a green corrosion inhibitor.

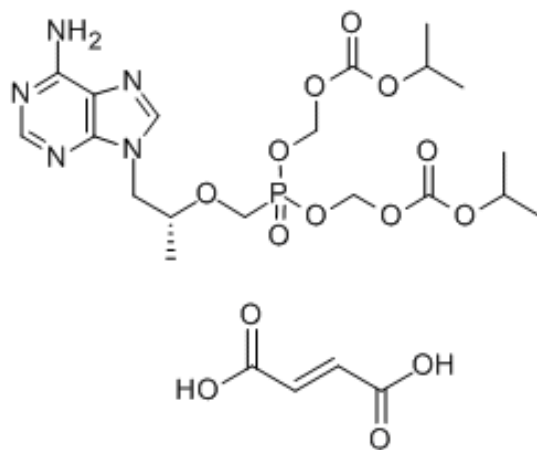


Figure 1. (9-[(R) 2[[bis [[(isopropoxycarbonyl)oxy]methoxy] phosphinyl] methoxy] propyl] adenine fumarate)

2. EXPERIMENTAL

2.1. Materials

The mild steel specimens, with composition (wt %) Fe 99.30%, C 0.076%, Si 0.026%, Mn 0.192%, P 0.012%, Cr 0.050%, Ni 0.050%, Al 0.023%, and Cu 0.135%, was cleaned successively with emery papers from 600 to 1200 mesh/in grade then washed with double distilled water, rinsed in acetone and finally dried in hot air blower. All experiments were carried out in unstirred solutions of 1M HCl which was prepared by dilution of analytical grade HCl (37%) in double distilled water. The mild steel specimens having exposed area $2.5 \times 2.0 \times 0.025\text{cm}^3$ were used for weight loss experiments and electrochemical measurements were carried out on a 7.5 cm long stem with exposed area of $1.0 \times 1.0\text{cm}^2$ and remaining portion were covered with commercially available lacquers.

2.2. Test solution

The test solutions of Tenvir were made by dissolving it in 1 M HCl solution and for dilution double distilled water was used.

2.3. Weight loss method

The weight loss measurements were carried out by standard method as described earlier [22]. The inhibition efficiency (η %) and surface coverage (θ) was calculated by using the following equations:

$$\eta\% = \frac{C_R - C_{R(i)}}{C_R} \times 100 \quad (1)$$

$$\theta = \frac{C_R - C_{R(i)}}{C_R} \quad (2)$$

where C_R and $C_{R(i)}$ are the corrosion rate values in absence and presence of Tenvir, respectively. The corrosion rate (C_R) of mild steel in acidic medium was calculated by using following equation:

$$C_R = \frac{W}{At} \quad (3)$$

where, W is weight loss of mild steel specimens (mg), A is the area of the specimen (cm^2) and t is the exposure time (h).

2.4. Electrochemical method

2.4.1. Electrochemical impedance spectroscopy

The EIS tests were performed at 308K in a three electrode assembly. The mild steel with 1cm^2 exposed areas used as working electrode, a saturated calomel electrode (SCE) was used as reference

electrode, and a high purity platinum sheet was used as the auxiliary electrode. All the electrochemical experiments were performed in absence and presence of different concentration of Tenvir in 1M HCl. The three electrode assembly connected to a Gamry Potentiostat/ Galvanostat (Model G-300) instrument. It is based on ESA 400 in a frequency range $10^{-2}\text{Hz} - 10^{-5}\text{Hz}$ under potentiodynamic conditions with amplitude of 10 mV peak to peak, using AC signal at E_{corr} . The experimental data were processed by Gamry Echem Analyst 5.0 software. The experiments were carried out after 30 minutes of immersion in the test solution without de-aeration and stirring. The inhibition efficiency was calculated from the charge transfer resistance values by using this equation:

$$\eta\% = \left(1 - \frac{R_{ct}}{R_{ct(i)}}\right) \times 100 \quad (4)$$

where, R_{ct}^i and R_{ct}^0 are the charge transfer resistances in presence and absence of Tenvir, respectively.

2.4.2. Potentiodynamic polarization

The electrochemical polarization behavior of mild steel specimens was study by recording the anodic and cathodic potentiodynamic curves. The potentiodynamic measurements performed in 1M HCl in absence and presence of different concentration of Tenvir by changing the electrode potential automatically from -250 to +250 mV vs. corrosion potential at a scan rate of 1 mV s^{-1} . The corrosion current density (I_{corr}) obtained by extrapolating the linear segments of cathodic and anodic polarization curves, from which inhibition efficiency was calculated using following formula.

$$\eta\% = \left(1 - \frac{I_{\text{corr}(i)}}{I_{\text{corr}}}\right) \times 100 \quad (5)$$

where, I_{corr} and $I_{\text{corr}(i)}$ are the corrosion current densities in absence and presence of Tenvir, respectively.

2.5. Surface investigation

The mild steel specimens having exposed area $1.0 \times 1.0 \times 0.025 \text{ cm}$ were immersed in 1M HCl for 3h in absence and presence of optimum concentration (400 ppm) of the Tenvir. After elapsed time mild steel specimens were taken out and their surface morphology were determined using Scanning Electron Microscopy (SEM) and elemental composition was determined by energy dispersive X-ray spectroscopy (EDX) using FEI Quanta 200F microscope.

3. RESULTS AND DISCUSSION

3.1. Weight loss measurements

3.1.1. Effect of concentration

Weight loss measurements were carried out at various concentrations of Tenvir. The variation of inhibition efficiency with concentration of Tenvir is shown in Figure 2(a). Various weight loss parameters such as percentage inhibition efficiency, surface and corrosion rate derived from weight loss experiment are given in the Table1.

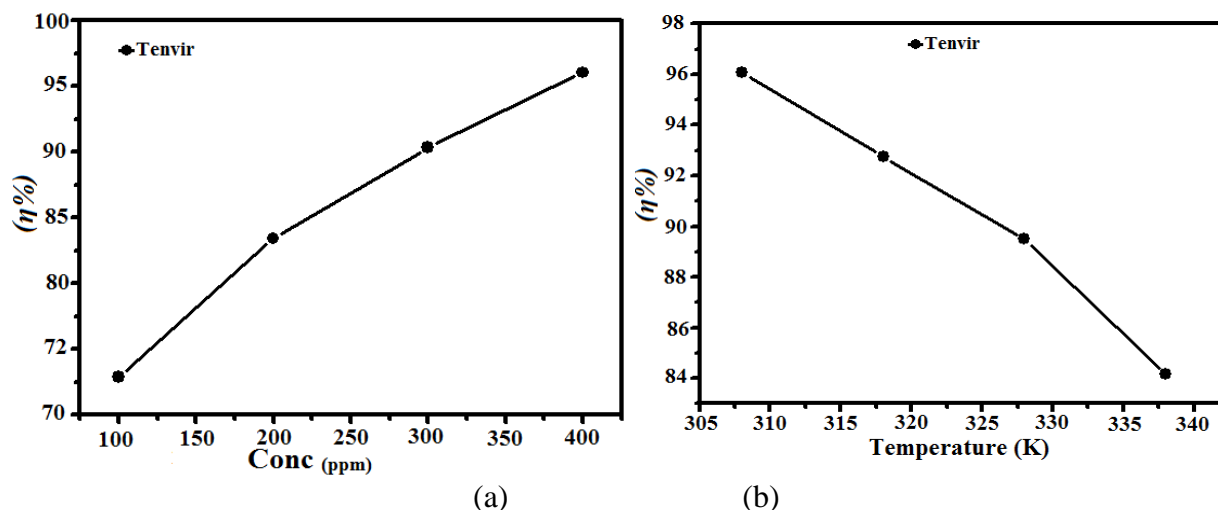


Figure2. (a) Inhibition efficiency of Tenvir at different concentrations (b) Inhibition efficiency of Tenvir at different temperatures

It is observed from the Table 1 that the inhibition efficiency increases with increase in concentration of Tenvir up to 400 ppm and further increase in concentration does not cause any significant change in the inhibition performance suggesting that 400 ppm is optimum concentration. The maximum inhibition efficiency (95.7%) was obtained at 400 ppm concentration. From the weight loss experimental results it is evident that both inhibition efficiency and surface coverage increase with Tenvir concentration.

Table 1. Corrosion rate and Inhibition efficiency (η %) for the mild steel in 1 M HCl in the absence and in the presence of different concentration of Tenvir

inhibitor	Concentration (ppm)	Corrosion rate (C_R mg cm ⁻² h ⁻¹)	Surface coverage (θ)	η%
Blank	0.0	7.66		
Tenvir	100	1.80	0.7631	76.31
	200	1.26	0.8342	83.42
	300	0.733	0.9035	90.35
	400	0.30	0.9605	96.05

3.1.2. Effect of temperature

To evaluate the effect of temperature on the inhibition efficiency of Tenvir, the weight loss measurements were performed on mild steel specimens in the temperature range of 308 to 338 K in absence and presence of optimum concentration. It is clear from Figure 2 (b) that on increasing temperature from 308 to 338 K, the inhibition efficiency decreases from 96.08% to 84.16%. This decrease in inhibition efficiency with temperature is due to desorption of adsorbed Tenvir from mild steel surface. The value of corrosion rate were calculated at each temperature and given in Table 2. The inspection of table 2 reveals that corrosion rate increases with increasing temperature.

Table 2. Variation of corrosion rate at different temperature in absence and presence of optimum concentration of Tenvir

Temperature	Corrosion rate (mg cm ⁻² h ⁻¹)	
	Blank	Tenvir
308	7.66	0.30
318	9.66	0.70
328	14.6	1.53
338	18.7	2.96

3.1.3 Thermodynamic activation parameters and adsorption isotherms

The mechanism of corrosion inhibition can be explained on basis of molecular adsorption behavior [23]. Several adsorption isotherms were tested to describe the adsorption behavior of Tenvir. The degree of surface coverage (θ) for different concentrations of Tenvir was evaluated from weight loss experiment. It is found that Tenvir obey Langmuir adsorption isotherm (Figure 3 (a)). Corrosion rate depend upon temperature and this dependency is given be Arrhenius equation and transition state equation [24].

$$\log(C_R) = \frac{-E_a}{2.303RT} + \log \lambda \tag{6}$$

$$C_R = \frac{RT}{Nh} \exp\left(\frac{\Delta S^*}{R}\right) \exp\left(-\frac{\Delta H^*}{RT}\right) \tag{7}$$

where E_a is the apparent effective activation energy, R is the general gas constant, T is the absolute temperature, λ is the Arrhenius pre-exponential factor, h is the Plank’s constant, N is the Avogadro’s number, ΔS^* is the entropy of activation and ΔH^* is the enthalpy of activation. The linear plot between $\log (C_R)$ vs. $1/ T$ and $\log (C_R/T)$ vs. $1/ T$ were performed. As shown in Figure 3 (b ,c) straight line obtained with a slope $-\Delta E_a/2.303 R$, $-\Delta H^*/ 2.303R$) and an intercept of $\log (R/Nh)+(\Delta S^*/ 2.303R)$, from which values of E_a , ΔH^* and ΔS^* were calculated respectively, and given in Table 3: The Figure 3 (b) represents the Arrhenius plot which is plotted between $\log C_R$ vs $1/T$ and Figure 3 (c) represent the transition state plot which is plotted between $\log C_R/T$ vs $1/T$. From Table 3, it is clear

that E_a in presence of Tenvir is higher (66.38 kJ mol⁻¹) as compare to blank acid solution (28.48 kJ mol⁻¹) this increase in the value of E_a in presence of Tenvir may be partially due to the physical adsorption that occur in the first step which is found during adsorption processes and partially due to desorption of adsorbed inhibitor molecules from mild steel surface [25].

Table 3. value of E_a , $-\Delta H^*$, ΔS^* in absence and presence of optimum concentration of Tenvir

Inhibitor	E_a	ΔH^*	ΔS^*
Blank	28.48	26.04	-148.9
Tenvir	66.38	63.70	-28.20

The positive sign of ΔH^* reflected the endothermic nature of mild steel dissolution in 1M HCl, which suggested the slow dissolution rate of mild steel in presence of Tenvir [26]. The shift towards positive value of entropies (ΔS^*) shows that the formation activated complex takes place in the rate determining step, representing dissociation rather than association, meaning that disorderness increases on going from reactants to the activated complex [27]

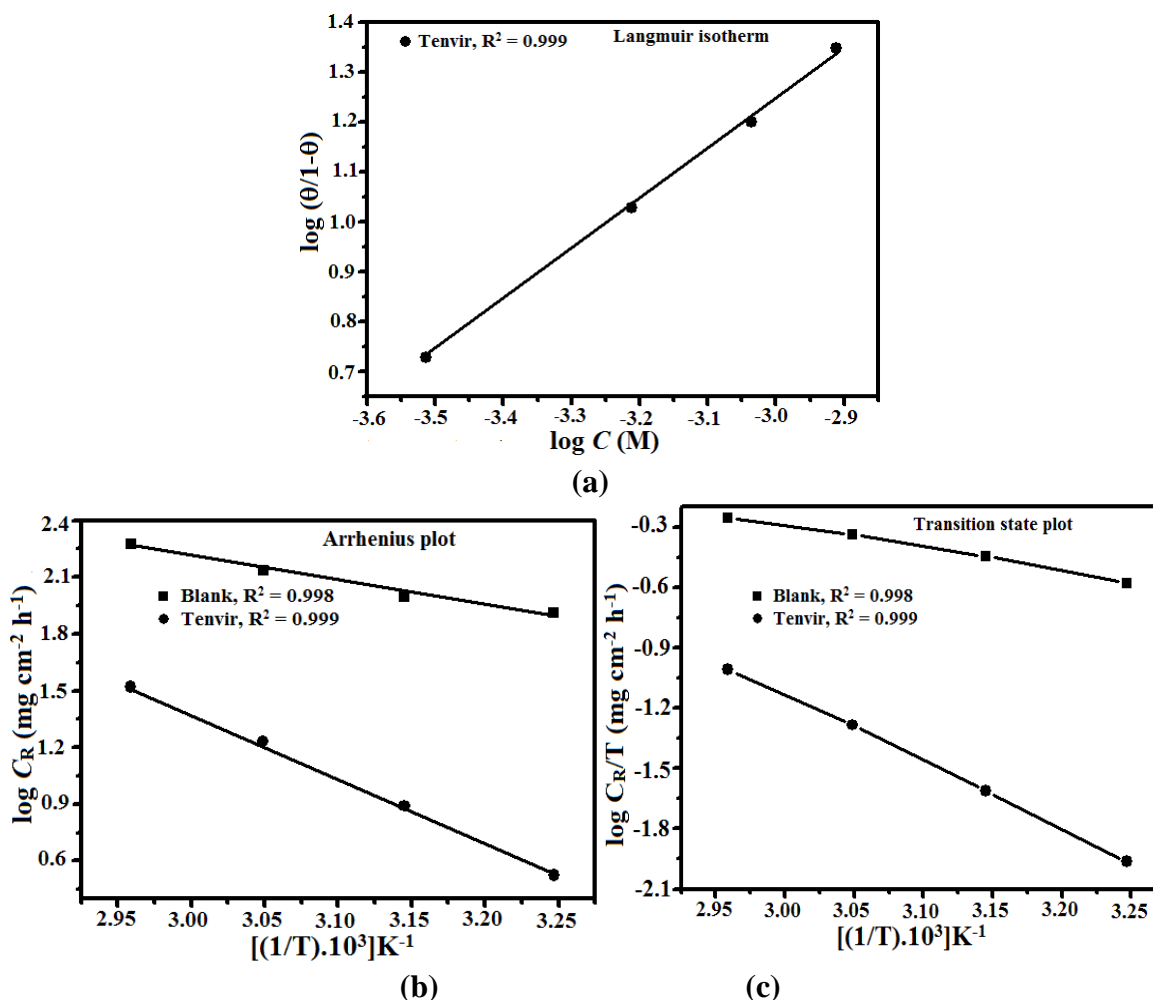


Figure 3. (a) Langmuir’s isotherm (b) Arrhenius plot (c) Transition state plot

The adsorption of inhibitor on the metal surface in acidic solutions involves two types of interactions one due to electrostatic interaction between charged inhibitor molecules and metal surface (physical adsorption) and other due to sharing of charges between inhibitor and vacant d- orbitals of the surface iron atoms (chemical adsorption). Various isotherms including Langmuir, Temkin and Freundlich were tested but Langmuir adsorption give the best fit having regression coefficient value very close to unity. The Langmuir isotherm can be represented by following equation:

$$\frac{C_{(\text{inh})}}{\theta} = \frac{1}{K_{(\text{ads})}} + C_{(\text{inh})} \quad (8)$$

where, $C_{(\text{inh})}$ is inhibitor concentration and K_{ads} is equilibrium constant for adsorption desorption process. The value of K_{ads} increases with increasing the concentration of inhibitor and decreases with increasing temperature. The standard free energy of adsorption depends upon the value of K_{ads} and this dependency can be expressed by following equation:

$$\Delta G_{\text{ads}}^{\circ} = -RT \ln(55.5K_{\text{ads}}) \quad (9)$$

$$\ln K_{\text{ads}} = \frac{-\Delta H_{\text{ads}}^{\circ}}{RT} + \text{constant} \quad (10)$$

The values of free energy of adsorption and adsorption constant were calculated and given in table 4. It is evident from the Table 4 that the value of K_{ads} decreased with increase in temperature indicating that adsorption of Tenvir on the mild steel surface was unfavorable at higher temperatures.

Table 4. Value of free energy of adsorption ($-\Delta G_{\text{ads}}$) and adsorption constant (K_{ads}) at various temperature

Temperature	$-\Delta G_{\text{ads}}$ (kJ mol ⁻¹)	K_{ads} (10 ⁴ M ⁻¹)
308	36.64	2.94
318	36.14	1.53
328	36.11	1.02
338	35.91	0.64

The negative values of ΔG_{ads} suggest that adsorption of inhibitor on mild steel surface is a spontaneous process. Generally, the values of ΔG_{ads} -20 kJ mol⁻¹ or less are associated with an electrostatic interaction between charged molecules and charged mild steel surface (physisorption) and those of -40 kJ mol⁻¹ or more negative involve charge sharing or transfer from the inhibitor molecules to the metal surface to form a coordinate covalent bond (chemisorption) [28]. In our present case the value of ΔG_{ads} ranges from 36.64 to 35.91 kJ mol⁻¹. This finding suggests that Tenvir is a mixed type inhibitor.

3.2 Electrochemical measurements

3.2.1. Electrochemical impedance spectroscopy

The electrochemical impedance nature of mild steel in 1M HCl in absence and presence of different concentration of Tenvir was studied by recording the Nyquist and Bode plots [Figure 4(a), (b)]. From the Nyquist plot it is clear that diameter of semicircle increases with increasing the concentration of Tenvir. Various impedance parameters such as R_s , R_{ct} , Y_0 , n , and C_{dl} were derived from the Nyquist plot and given in Table 5.

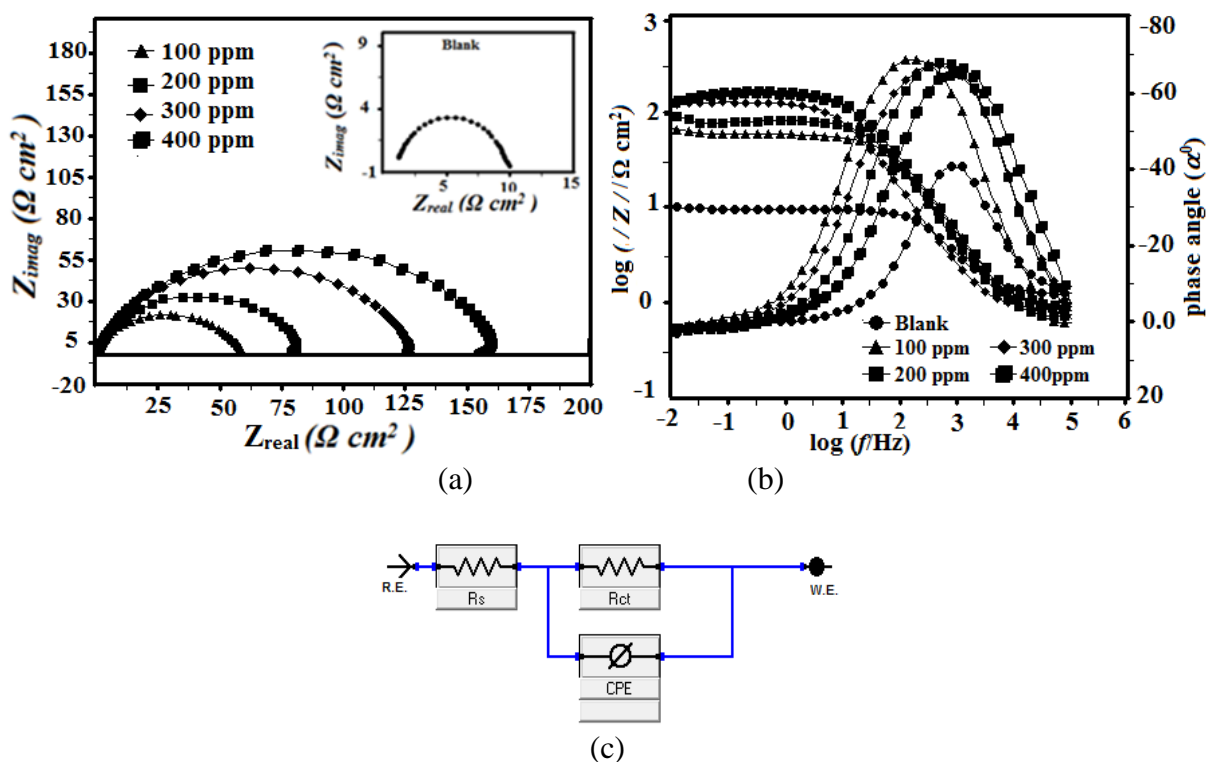


Figure 4. (a-c). (a) Nyquist plot for mild steel in 1M HCl in absence and presence of different concentration of Tenvir (b) Bode ($\log f$ vs. $\log |Z|$) and phase angle ($\log f$ vs. α) plots of impedance spectra for mild steel (c) Equivalent circuit used to fit the EIS data for mild steel in 1M HCl

The equivalent circuit shown in Figure 4(c) was used to analyze the all impedance data. The double layer capacitance (C_{dl}) was calculated using following equation [29]:

$$C_{dl} = \frac{Y \omega^{n-1}}{\sin(n(\pi / 2))} \tag{11}$$

where Y^0 is the CPE coefficient, n is the CPE exponent (phase shift), ω is the angular frequency. The ω_{max} represents the frequency at which the imaginary component reaches a maximum. It is the frequency at which the real part (Z_{real}) is midway between the low and high frequency x-axis intercepts.

Table 5. Electrochemical parameters calculated from EIS measurements for mild steel electrode in 1 M HCl in absence and presence of different concentration of Tenvir.

Inhibitor	Concentration (ppm)	R_s	R_{ct}	N	Y^0	C_{dl}	$\eta\%$
Blank	.0	1.12	9.58	0.827	249.8	106.2	--
Tenvir	100	0.581	42.1	0.847	106.2	43.73	77.24
	200	0.696	64.3	0.868	125.5	49.69	85.10
	300	0.851	112.7	0.865	229.3	48.78	91.32
	400	0.842	159.7	0.837	129.5	41.16	94.00

It is clear from Table 5 that value of R_{ct} increases from $9.58 \Omega \text{ cm}^2$ (in absence of Tenvir) to $159.7 \Omega \text{ cm}^2$ on addition of 400ppm of Tenvir. The value of C_{dl} decreases from $106.2 \mu\text{F cm}^{-2}$ (in absence of Tenvir) to $41.16 \mu\text{F cm}^{-2}$ on addition of 400 ppm concentration of Tenvir. The decrease in capacitance (C_{dl}) on addition of Tenvir may be due to increase in local dielectric constant and/or may be due to increase in the thickness of the double layer, showing that Tenvir inhibited mild steel corrosion in by adsorbing at metal/acid interfaces [30].

Figure 4 (b) represent the Bode plot in absence and presence of different concentration of Tenvir. In intermediate frequency region, a linear relationship between $\log |Z|$ vs $\log f$ with a slope near -1 and the phase angle approaching -80° has been observed. An ideal capacitive behavior would be the result if a slope value attained -1 and a phase angle value attained -90° . From Bode plots, it is observed that value of $\log |Z|$ and phase angle (α°) decreases at high frequency region. This decrease is due to solution resistance between reference (saturated calomel) and working electrodes (mild steel). This deviation from ideal capacitive (with slope -1 and phase angle -90) behavior at intermittent frequencies may be related to dawdling dissolution rate of mild steel in presence of dendrimers with time.

3.2.2. Potentiodynamic polarization measurements

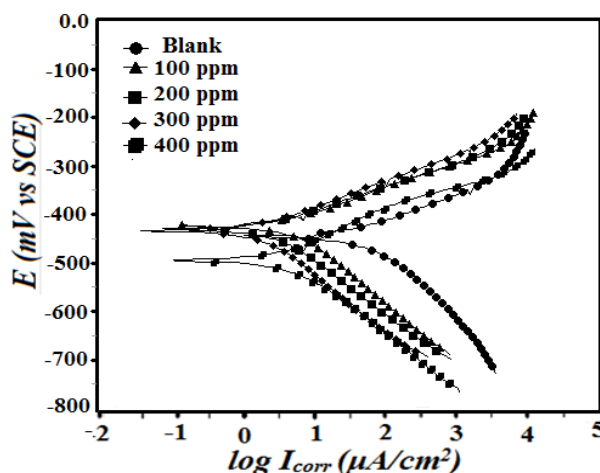


Figure 5. Potentiodynamic polarization curves for mild steel in 1M HCl in absence and presence of different concentration of Tenvir

The potentiodynamic polarization measurements were carried out in order to gain knowledge concerning the kinetics of the cathodic and anodic reactions. Polarization curves of the mild steel electrode in 1 M HCl in absence and at different concentrations of Tenvir is shown in Figure 5.

The values of various potentiodynamic polarization parameters namely corrosion potential (E_{corr}) corrosion current density (I_{corr}), cathodic and anodic Tafel slope (β_c and β_a , respectively) and corresponding inhibition efficiency (η %) obtained by extrapolation of the Tafel lines were given in Table 6.

Table 6. Tafel Polarization parameters for mild steel in 1 M HCl solution containing different concentrations of Tenvir

Inhibitor	Concentration(ppm)	E_{corr}	I_{corr}	β_a	β_c	$\eta\%$	θ
Blank	0.0	-445	1150	70.5	114.6	----	---
Tenvir	100	-405	285.3	104.8	132.4	75.19	0.7519
	200	-424	176.3	59.3	97.4	84.66	0.8466
	300	-431	134.3	70.5	135.4	88.32	0.8832
	400	-434	65.8	75.5	145.2	94.27	0.9427

From Table it is clear that inhibition efficiency increases with increasing concentration and maximum efficiency was obtained was 95.7% at 400 ppm concentration. The value of E_{corr} is related to the potentiodynamic polarization nature of Tenvir in 1M HCl. Generally, if the value of E_{corr} is greater than 85 mV/ SCE the inhibitor can be classified as cathodic or anodic type and however, if the value of E_{corr} is lower than 85 mV/SCE the inhibitors can be classified as mixed type. In our present study addition of inhibitor did not cause any significant change in E_{corr} suggesting that Tenvir is a mixed type inhibitor [31]. The adsorbed protective film of inhibitor on the mild steel surface retarded corrosion by blocking the reaction sites of the mild steel. In this way, actual surface area available for H^+ ions is decreased while the actual reaction mechanism remains unaffected.

3.3. Surface investigation

3.3.1. Scanning electron microscope (SEM) analysis

The SEM micrographs of mild steel specimens after 3 h immersion time in 1 M HCl in absence and presence of optimum concentration of Tenvir is shown in Figure 6 (a-b).

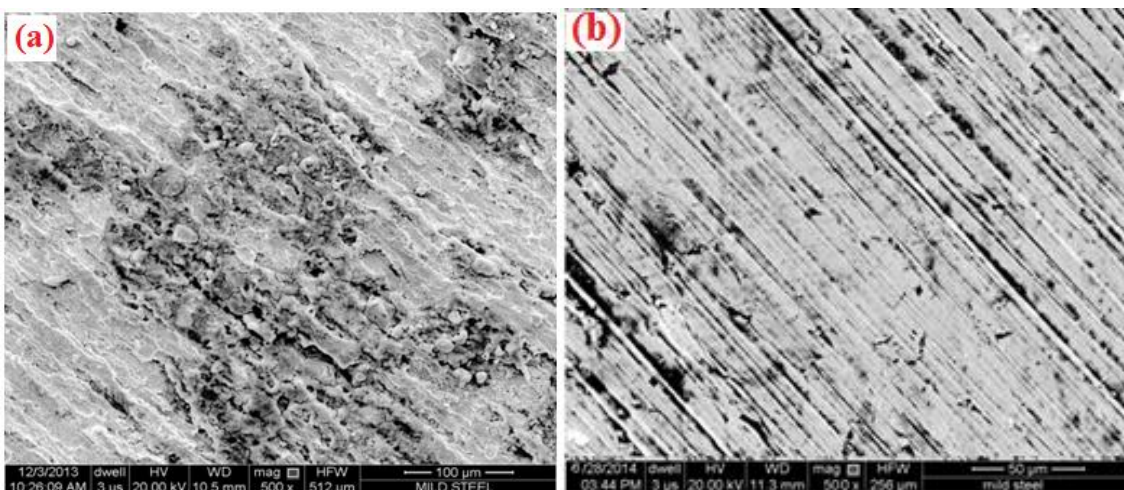


Figure 6. (a-b). SEM micrographs of mild steel surfaces (a) un inhibited 1M HCl (b) in presence of Tenvir

The Figure 6 (a) represents the SEM image of mild steel in absence of Tenvir which is characterized by very rough surface with pits and cracks. This finding suggests that mild steel surface strongly damaged by acidic solution in absence of Tenvir. The Figure 6 (b) represents the SEM micrographs of mild steel in presence of optimum concentration of Tenvir. From figure it is clear that surface morphology significantly smoothed in presence of the Tenvir which suggests that mild steel surface were fully covered with the Tenvir molecules and a protective Tenvir film was formed. This finding supports the weight loss, EIS and polarization results.

3.3.2. Energy dispersive X-ray spectroscopy (EDX) analysis

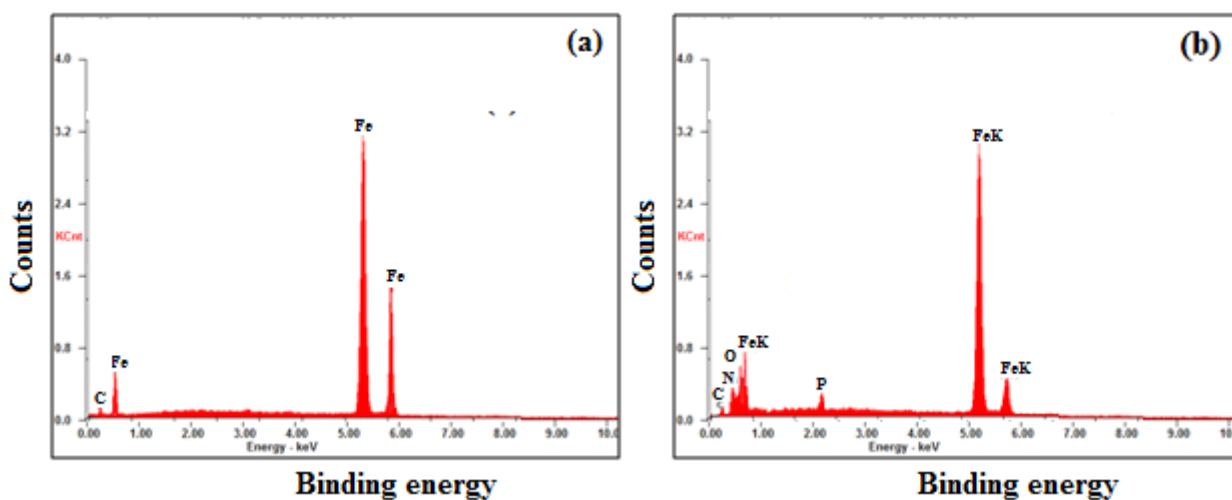


Figure 7. (a-b). EDX spectra of mild steel surfaces (a) in un inhibited 1M HCl (b) in presence of Tenvir

The purpose of this study is to conform the finding of weight loss and electrochemical results. The EDX spectra of mild steel specimens after 3 h immersion time in 1M HCl in absence and presence of the Tenvir is shown in Figure 7 (a-b) and percentage elemental composition obtained from EDX spectra is given in table 7.

In EDX spectrum of uninhibited mild steel specimen (Figure 7a), the peak of O is absent which confirms the dissolution of air-formed oxide film and free corrosion of bare metal. However, EDX spectra of mild steel in presence of Tenvir [Figure 7 (b)] show additional peaks for oxygen, nitrogen and phosphorus which due to presence of Tenvir on mild steel surface.

Table 7. Percentage atomic contents of elements obtained from EDX spectra of tenvir at optimum concentration

Inhibitor	Fe	C	N	O	P
Blank	63.09	36.10	---	---	----
Tenvir	56.62	22.27	5.46	13.76	1.79

From the EDX spectra in inhibited solution, it is clear that the peaks for Fe are significantly suppressed relative to the uninhibited mild steel sample. The suppression of Fe lines occurs due to the overlying Tenvir film on mild steel surface. The Energy dispersive X-ray spectroscopy further supports the formation of protective film of Tenvir on mild steel surface.

3.4. Mechanism Of Corrosion Inhibition

The corrosion inhibition of mild steel in 1M HCl by Tenvir can be explained on the basis of molecular adsorption on to the mild steel surface. The adsorption of the inhibitor on the mild steel surface influenced by nature of charge on metal surface and chemical structure of the inhibitors. This charge development on metal surface is due to electric field which generates at the metal/electrolyte interface in acid solution. It is well reported that mild steel is positively charged in acid solution with respect to the potential of zero charge (PZC) [32].

The Tenvir can be adsorb on the metal/acid solution interface by (I) electrostatic interaction of protonated Tenvir molecules with already adsorbed chloride ions (physisorption), (II) unshared electron pairs of heteroatoms and vacant d-orbital of Fe surface atoms (chemisorption), or (III) interaction of d-electron of iron surface atom to the vacant orbital of inhibitor molecule (retro donation). In the aqueous acidic solution the Tenvir can be adsorb on mild steel through protonated heteroatoms and previously adsorb chloride ions. In the first step of adsorption the protonated form of the Tenvir start competing with H^+ ions for electrons. However, after releasing the H_2 gas the positively charged inhibitor comes in its neutral form and the heteroatoms with free lone pair of electrons adsorb by donating its electrons to the d-orbitals of the surface iron atoms. The accumulation of extra negative charge on mild steel surface render it to more negative and to relieve the metal from the excessive negative charge the electrons might be transferred from the d-orbital to the vacant pi-antibonding

molecular orbitals of the Tenvir (retro donation). Thus Tenvir can adsorb on the mild steel surface by following ways:

- (a) Electrostatic interaction between the charged molecules and charged metal;
- (b) Interaction of π -electrons with the metal;
- (c) Interaction of unshared pair of electrons in the molecule with the metal; and
- (d) The combination of the all the effects [33, 34].

4. CONCLUSIONS

- (1) The Tenvir is good corrosion inhibitor for mild steel corrosion in 1 M HCl solution.
- (2) The inhibition efficiency of Tenvir increases with increase in concentration and maximum efficiency (95.7%) was observed at 400 ppm concentration.
- (4) The adsorption of Tenvir on mild steel surface obeys the Langmuir adsorption isotherm.
- (5) The inhibiting efficiencies obtained by polarization, *EIS* and weight loss measurements are in good agreement.
- (6) The negative sign of the ΔG_{ads} indicates that the adsorption of Tenvir on the mild steel surface in 1 M HCl is spontaneous process.

References

1. I. Ahamad, R. Prasad, M.A. Quraishi, *Corros. Sci.*, 52 (2010) 933.
2. A. Singh, V. K. Singh, M. A. Quraishi, *Arab. J. Sci. Eng.*, 38 (2013) 85.
3. G. Schneider, H. Bohm, *Drug. Discov. Today.*, 76 (2002) 64.
4. T.I. Oprea, *Molecules.*, 7, (2002) 51.
5. C.B. Verma, M.A., Quraishi, E.E. Ebenso *Int. J. Electrochem. Sci.*, 8 (2013) 12238.
6. D.J. Newman, G.M. Cragg, *J. Nat. Prod.*, 70 (2007) 461.
7. A.L. Harvey, *Drug Discov. Today.*, 13 (2008) 894.
8. S. Struck, U. Schmidt, B. Gruening, I.S. Jaeger, J. Hossbach, R. Preissner, *Genome Inform.*, 20 (2008) 231.
9. O.V. Enick, Do pharmaceutically active compounds have an ecological impact, M.Sc. Thesis, Simon Fraser University, Burnaby, (2006)
10. M.A. Quraishi, S. K. Shukla. *J. Appl. Electrochem.*, 39 (2009) 1517.
11. M.A. Quraishi, S. K. Shukla, *Mater. Chem. Phys.*, 120 (2010) 142.
12. M.A. Quraishi, S. K. Shukla, *Corros. Sci.*, 52 (2010) 314.
13. I. Ahamad, R. Prasad, M. A. Quraishi, *Corros. Sci.*, 52 (2010) 3033.
14. I. Ahamad, R. Prasad, M. A. Quraishi, *J. Solid State Electrochem.*, 14 (2010) 2095.
15. M. J. Reddy, C. B. Verma, E..E Ebenso, K. K. Singh, M. A. Quaraisi, *Int. J. Electrochem. Sci.*, 9 (2014) 4884.
16. C. B. Verma, M. J. Reddy, M. A. Quraishi, *Anal. Bioanal. Electrochem.*, 6, (2014) 515.
17. M. Abdallah, *Corros. Sci.*, 44 (2002) 717.
18. A. Singh, A. K. Singh, M. A. Quraishi, *the Open Electrochem. J.*, 2 (2010) 43.
19. I. Ahamad, M. A. Quraishi, *Corros. Sci.*, 52 (2010) 651.
20. N. O. Eddy, S. A. Odoemelam, P. Ekwumemgbo, *Scientific Research and Essay.*, 4 (2009) 33.
21. C. B. Verma, M.A. Quraishi, *IJIRSET.*, 3 (22014) 14601.

22. C.B. Verma, M.A. Quraishi, E.E. Ebenso. *Int. J. Electrochem. Sci.*, 8 (2013) 7401.
23. P. Sounthari, A. Kiruthika, J. Saranya, K. Parameswari, S. Chitra, *J. Adv. Chem.*, 10 (2014) 2126.
24. M. Yadav, D. Behera, S. Kumar, R. R. Sinha, *Ind. Eng. Chem. Res.* 52 (2013) 6318.
25. N.O. Eddy, U. J. Ibok, E. E. Ebenso, A. El.Nemr, E.S.H. El Ashry, *J. Mol. Model.*; 15 (2009) 1085.
26. M. Yadav, D. Behera, S. Kumar, R. Ranjan Sinha, *Ind. Eng. Chem. Res.*, 2013, 52, 6318.
27. A. K. Singh, *Ind. Eng. Chem. Res.*, 51 (2012) 3215.
28. C. B. Verma, M. J. Reddy, M. A. Quraishi, *Anal. Bioanal. Electrochem.*, 6 (2014) 321.
29. A. K. Singh, M. A. Quraishi, *Corros. Sci.*, 52 (2010) 152.
30. S.H. Kumar, S. J. Karthikeyan, *Mater. Environ. Sci.*, 3 (5) (2012) 925.
31. C. B. Verma M.A. Quraishi, *IJIRSET.*, 3 (7) (2014) 14601.
32. D. K. Yadav , M. A. Quraishi, *Ind. Eng. Chem. Res.*, 51 (2010) 8194.
33. X. Li, S. Deng, H. Fu, T. Li, *Electrochim. Acta.*, 54 (2009) 4089.
34. Q. B. Zhang, Y. X. Hua, *Electrochemical Acta.*, 54 (2009) 1881.

© 2015 The Authors. Published by ESG (www.electrochemsci.org). This article is an open access article distributed under the terms and conditions of the Creative Commons Attribution license (<http://creativecommons.org/licenses/by/4.0/>).